ADVANCES IN ATMOSPHERIC SCIENCES, VOL. 30, NO. 4, 2013, 1117–1128

Revealing the Effects of the El Niño-Southern Oscillation on Tropical Cyclone Intensity over the Western North Pacific from a Model Sensitivity Study

ZHOU Yang*[1] (周 洋), JIANG Jing[1] (江 静), Youyu LU[2] (鹿有余), and HUANG Anning[1] (黄安宁)

[1] *School of Atmospheric Sciences, Nanjing University, Nanjing* 210093

[2] *Fisheries and Oceans Canada, Bedford Institute of Oceanography, Dartmouth, Nova Scotia, B2Y 4A2, Canada*

(Received 31 May 2012; revised 10 September 2012; accepted 21 September 2012)

ABSTRACT

Five sets of model sensitivity experiments are conducted to investigate the influence of tropical cyclone (TC) genesis location and atmospheric circulation on interannual variability of TC intensity in the western North Pacific (WNP). In each experiment, bogus TCs are placed at different initial locations, and simulations are conducted with identical initial and boundary conditions. In the first three experiments, the specified atmospheric and SST conditions represent the mean conditions of El Niño, La Niña, and neutral years. The other two experiments are conducted with the specified atmospheric conditions of El Niño and La Niña years but with SSTs exchanged. The model results suggest that TCs generated in the southeastern WNP incurred more favorable environmental conditions for development than TCs generated elsewhere. The different TC intensities between El Niño and La Niña years are caused by difference in TC genesis location and low-level vorticity (VOR). VOR plays a significant role in the intensities of TCs with the same genesis locations between El Niño and La Niña years.

Key words: tropical cyclone intensity, western North Pacific, ENSO, MM5, low level vorticity

Citation: Zhou, Y., J. Jiang, Y. Y. Lu, and A. N. Huang, 2013: Revealing the effects of the El Niño-Southern oscillation on tropical cyclone intensity over the western North Pacific from a model sensitivity study. *Adv. Atmos. Sci.*, **30**(4), 1117–1128, doi: 10.1007/s00376-012-2109-5.

1. Introduction

Tropical cyclone (TC) activity over the western North Pacific (WNP) is a complicated issue. This activity is modulated by atmospheric or oceanic variability (or both) on various time scales, for example, by the Madden-Julian Oscillation (MJO) on intraseasonal time scale (e.g., Sobel and Maloney, 2000; Huang et al., 2011), by the El Niño-Southern Oscillation (ENSO) on interannual time scale (e.g., Chan, 1985; Chen et al., 1998, 2004), and by long-term oceanic variations on interdecadal time scale (e.g., Matsuura et al., 2003; Chan, 2008; Wang and Clark, 2010). Because of its particular concern to the public, many researchers have dedicated their efforts to investigating the reasons for the interannual variability of TCs.

On interannual time scale, the effects of ENSO on TC activity in the WNP have been the focus of many studies. Through cross-spectral analysis, Chan (1985) found that TC activity and the Southern Oscillation show significant coherence in spectral peak, with a period of 3 to 3.5 years. Using a high-resolution coupled atmosphere-ocean model, Iizuka and Matsuura (2008) suggested that the annual number of TCs is below normal during the following years of El Niño and above normal during the years before El Niño. However, while the correlation between ENSO and the annual total of TCs is not significant (Lander, 1993, 1994), the displacement of annual location of TC genesis in the WNP is associated with ENSO. In El Niño years, TCs are generated mostly in the southeast quadrant of the WNP, whereas in La Niña years, TCs are generated mostly in the northwest quadrant (Wang and Chan, 2002; Camargo et al., 2007a). Chan (1985) considered the displacement to be a consequence of the shifts of tropical atmospheric circulation; under El Niño condi-

*Corresponding author: ZHOU Yang, yangzhou@nju.edu.cn

tions, an anomalous Walker circulation is set up with upward current in the central equatorial Pacific and downward current in the western equatorial Pacific. Chen et al. (1998) suggested that the extension of the monsoon trough across 150°E influences the eastward displacement of the TC genesis locations and that the retreat of the monsoon trough influences the westward displacement of TC genesis. Wang and Chan (2002) attributed the eastward displacement of TC genesis location to the increase of the low-level vorticity generated by the equatorial westerly associated with El Niño. Generally, ENSO modulates atmospheric circulation, which influences the TC genesis location in the WNP.

In addition to TC genesis, ENSO also influences TC intensity in the WNP. Recently, Camargo and Sobel (2005) revealed that the accumulated cyclone energy of TCs in the WNP is positively correlated with the ENSO, and TCs in El Niño years are stronger and of longer duration than TCs in La Niña years. TCs that occur during El Niño years tend to form farther eastward with longer over-water tracks that contribute to increased intensity. Chan and Liu (2004) suggested that the interannual variation of TC intensity (as well as the annual number of TCs) in the WNP is not related to the variability of local SST but to the variability of atmospheric circulation. The results of these studies indicate that ENSO influences TC genesis location, which is related to TC intensity. In addition, ENSO-modulated atmospheric circulation affects TC intensity by providing suitable (or unsuitable) environments. In this study, model sensitivity experiments are used to explore the "separate" influence of the TC genesis location and the atmospheric circulation on TC intensity in the WNP. The experiments are designed to examine differences in TC intensity during neutral, El Niño, and La Niña conditions. (The influence of the atmospheric circulation on the genesis of a cyclonic vortex is not considered in the experiments.)

In section 2, data and the model experiments are described. Section 3 presents the analysis of the model results. Section 4 provides discussions and conclusions.

2. Data and model experiments

2.1 *Data*

The TC track and intensity of observations during June–November 1965–2009 in the WNP are obtained from the US Joint Typhoon Warning Center (JTWC). TCs generated in the area of 2.5°–22.5°N, 117.5°–172.5°E are studied.

The selection of El Niño, La Niña, and neutral years is based on the ENSO index of 1965–2009, which is obtained from the US National Oceanic and Atmospheric Administration/Climate Prediction Center (NOAA/CPC, http://www.cpc.noaa.gov). This index has been defined according to SST in Niño3.4 region (5°S–5°N, 120°–170°W; e.g., Trenberth, 1997; Pielke Jr and Landsea, 1999). An El Niño year is identified when the anomaly of the Niño3.4 SST during July–September of that year is above 0.5°C with reference to SST average during July–September of 1971–2000. A La Niña year is identified when the anomaly of the Niño3.4 SST during July–September of that year is below −0.5°C. The remaining years are considered neutral years. During 1965–2009, there are 12 El Niño years, 9 La Niña years, and 24 neutral years. The El Niño years are 1965, 1972, 1982, 1986, 1987, 1991, 1994, 1997, 2002, 2004, 2006 and 2009. The La Niña years are 1970, 1971, 1973, 1974, 1975, 1985, 1988, 1998, and 1999.

Model input is derived from the reanalysis data (R1, 6-h intervals) of the US National Centers for Environmental Prediction/ National Center for Atmospheric Research (NCEP/NCAR, http://dss.ucar.edu; Kalnay et al., 1996; Kistler et al., 2001). The reanalysis dataset has a 2.5°×2.5° horizontal grid, 17 pressure levels, and a 192×94 Gaussian grid on the ground. To explore the effects of the time-mean circulation on TC intensity, the data during June–November 1965–2009 are separated into three groups according to the definition of El Niño, La Niña, and neutral years and then they are averaged according to time. The time mean fields are used for the initial and boundary conditions of model simulations.

When the reanalysis fields are averaged, TC signals are included, but the signals in the 6-h reanalysis fields are weaker than that in observations because of the coarse horizontal resolution. Taking the 10-m wind speed ($V_{10} = \sqrt{u_{10}^2 + v_{10}^2}$) as an example, we calculate (1) the V_{10} average during June–November 1965–2009 (denoted by $V_{10\mathrm{Total}}$), and (2) the V_{10} average of the same period but excluding the data within a radius of 5° around the TC centers (denoted by $V_{10\mathrm{NTC}}$). The TC centers are defined according to the best tracks of the JTWC. The above computation is conducted for every reanalysis grid in the WNP. We find that the maximum value of $(V_{10\mathrm{Total}} - V_{10\mathrm{NTC}})/V_{10\mathrm{Total}}$ is only 0.03 (figure not shown). Thus, the difference between the mean fields with and without the data around active TCs can be ignored.

2.2 *Model experiments*

The Mesoscale Model version 5 (MM5) developed by the US Pennsylvania State University and NCAR is used in this study. This model has been extensively used to simulate the structure and evolution of TCs (e.g., Liu et al., 1997, 1999) and to study the influence

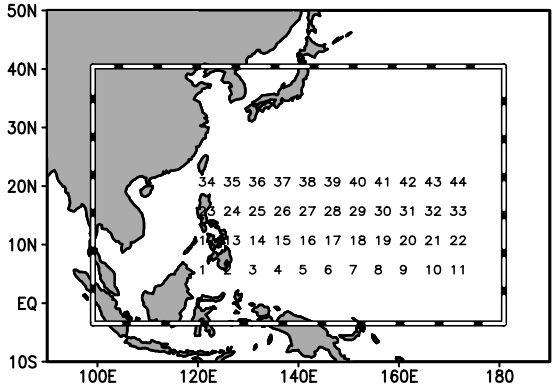

Fig. 1. Model domain (surrounded with dash lines) and 44 initial positions of bogus TCs (spaced by 5° and marked with numbers) in each experiment (Table 1).

of environmental factors on TC intensities (e.g., Frank and Ritchie, 1999, 2001; Wong and Chan, 2004).

Figure 1 shows the model domain (3.4°S–40.4°N, 99.1°E–179.1°W) of Mercator projection. The model has a 90×90-km horizontal grid on 23 sigma levels. The Betts-Miller cumulus parameterization (Betts, 1986; Betts and Miller, 1986, 1993; Janjic, 1994), the simple ice moisture scheme (Dudhia, 1989), and the Hong-Pan planetary boundary layer scheme (Hong and Pan, 1996) are used.

Five sets of model experiments with differences in initial fields and boundary conditions are conducted (Table 1). The first three experiments (NANS, EAES, and LALS) are defined with initial fields and boundary conditions with respect to neutral, El Niño, and La Niña years, respectively. The fourth, denoted by EALS, uses a combination of the atmospheric fields of El Niño years and the SST of La Niña years. The fifth, denoted by LAES, uses a combination of the atmospheric fields of La Niña years and the SSTs of El Niño years.

In each experiment, there are 44 TC simulations (Table 1), for a total of 220 simulations. At the beginning of each simulation, a bogus TC with a radius of 200 km and maximum wind speed of 5 m s^{-1} is placed at one of the 44 locations (Fig. 1). Each TC is simulated for 15 days from the starting location, and the output is saved at 3-h intervals. The details of the TC bogussing method can be found in the report by Lownam and Davis (2001). The locations in Fig. 1 are spaced by 5° in the area of 5°–20°N, 120°–170°E. Thus, the 44 simulations in each experiment represent the evolution of TCs from 44 different genesis locations, but under the same mean atmospheric and oceanic conditions.

Table 1. Five experiments represent conditions of neutral (NANS), El Niño (EAES), La Niña (LALS), combination of El Niño atmospheric circulation with La Niña SST (EALS), and combination of La Niña atmospheric circulation with El Niño SST (LAES).

Experiments	Mean Atmospheric Circulation	Mean SST
NANS	Neutral (NA)	Neutral (NS)
EAES	El Niño (EA)	El Niño (ES)
LALS	La Niña (LA)	La Niña (LS)
EALS	El Niño (EA)	La Niña (LS)
LAES	La Niña (LA)	El Niño (ES)

3. Model results

3.1 *Relationship between TC intensities and TC genesis locations*

Modeled TC intensities under the mean environmental conditions are analyzed first. At each time interval of model output (3 h), modeled TC intensity is defined as the maximum wind speed (at 10 m) around the TC center, which is located according to the minimum sea level pressure of the TC. Modeled TC intensity during the 15-day simulation is defined as the maximum value of the instantaneous intensities.

Figure 2 shows the statistics of the 220 modeled TC intensities. The TC intensity ranges (Fig. 2a) in the experiments with the same atmospheric circulation are quite similar (EAES vs. EALS and LALS vs. LAES). The variance of the TC intensities under El Niño atmospheric conditions (EAES and EALS) is larger than the variance under the La Niña conditions (LALS and LAES). The standard deviations (SD) are 6.1 m s^{-1} (EAES), 4.1 m s^{-1} (LALS), 6.1 m s^{-1} (EALS), 4.6 m s^{-1} (LAES), and 5.2 m s^{-1} (NANS). The standard deviation of the 220 modeled TC intensities is 5.4 m s^{-1}. The mean TC intensities (Fig. 2a, blue asterisks) under El Niño and neutral atmospheric conditions (EAES, EALS, and NANS) are smaller than those intensities under La Niña atmospheric conditions (LALS and LAES), but the differences are not significant. The average of the 220 TC intensities is 31.6 m s^{-1}. The weak TCs ($\leqslant$31.6–5.4 m s^{-1}) in EAES, EALS, and NANS are more than those of TCs in LALS and LAES (Fig. 2b; TC frequencies of EALS and LAES are not shown). However, the strong TCs ($\geqslant$31.6+5.4 m s^{-1}) under El Niño atmospheric conditions are more frequent than those TCs under the La Niña atmospheric conditions. There are more TCs with the intensities within 1 SD under La Niña atmospheric conditions.

Figure 3 shows the spatial distribution of the intensity anomalies of the 220 TCs. An anomaly is defined as the standardized intensities of the 220 TCs. If a TC has a positive intensity anomaly, a solid circle is

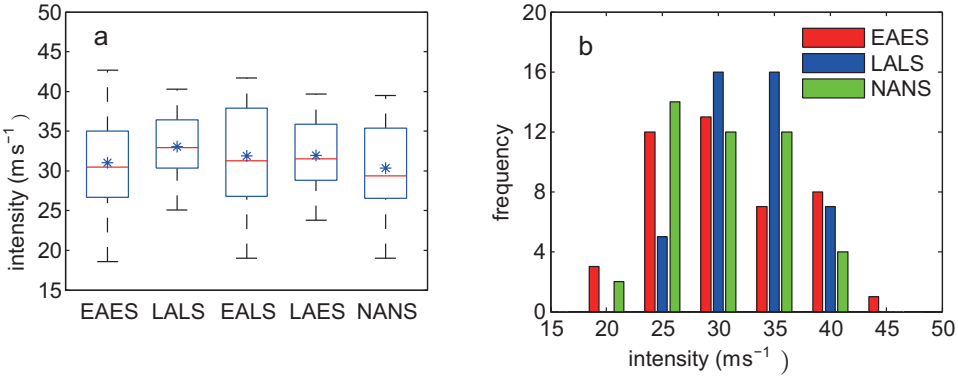

Fig. 2. (a) Box plot of the modeled TC intensities in each experiment. The central red line indicates the median of TC intensities; the upper and bottom edges of the blue box are the 75th and 25th percentiles, respectively. The black dashed line extends to the most extreme TC intensities, but outliers are not considered. The blue asterisk represents the mean TC intensity of each experiment. The x-axis and y-axis represent five experiments and TC intensity respectively. (b) TC intensity-frequency histogram for EAES, LALS, and NANS. The x-axis and y-axis represent TC intensity and frequency respectively.

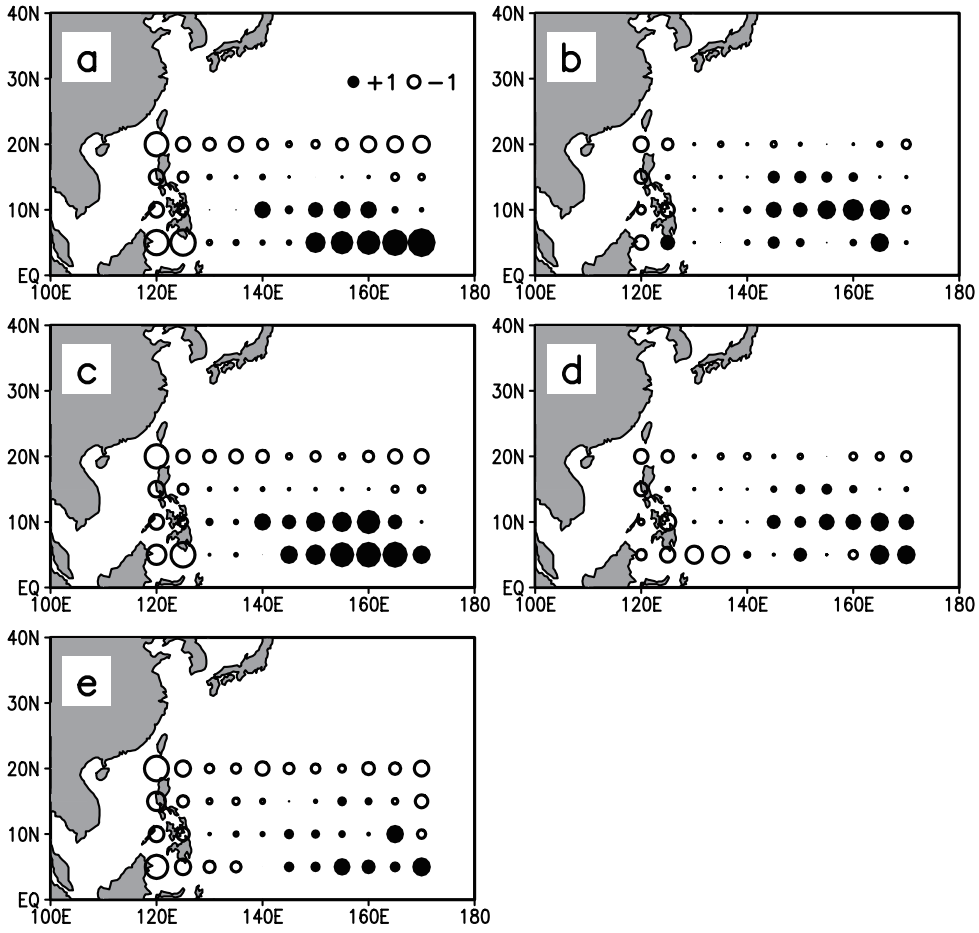

Fig. 3. TC intensity anomalies (standardized TC intensities) from model experiments, including (a) EAES, (b) LALS, (c) EALS, (d) LAES, and (e) NANS. A solid circle indicates that the intensity of a TC is stronger than the mean intensity and an open circle indicates that the intensity of a TC is weaker than the mean intensity (see text for details). The sizes of the circles represent the magnitudes of the anomalies. The legends in panel (a) show one positive (negative) standard deviation.

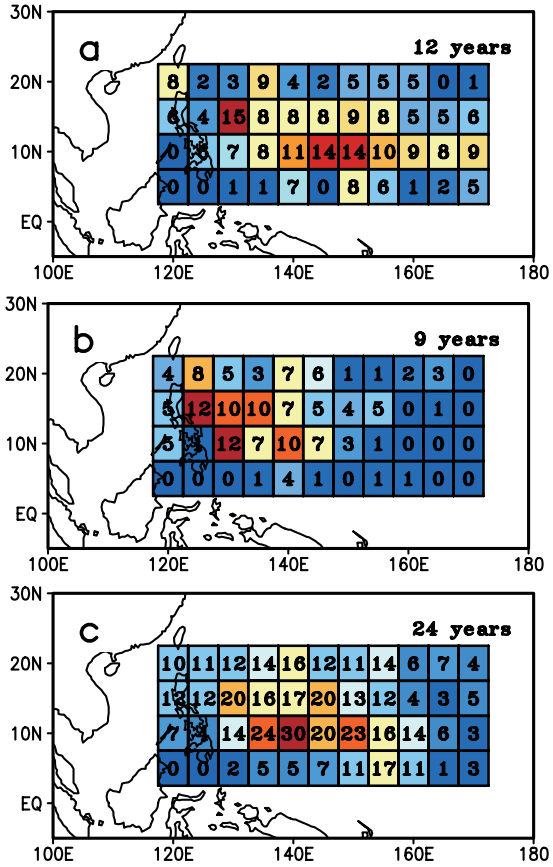

Fig. 4. TC genesis numbers of observations (see text for details). Under (a) El Niño, (b) La Niña, and (c) neutral conditions, each number is in a $5^\circ \times 5^\circ$ box (the centers of the locations are shown in Fig. 1). There are 12 El Niño years, 9 La Niña years, and 24 neutral years during 1965–2009, and the genesis rate in each box is the genesis number divided by the number of years under each of the conditions.

marked at the initial location of this TC, and if a TC has a negative intensity anomaly, an open circle is marked at the initial location of this TC. The size of the circle represents the magnitude of the anomaly. The model results suggest that TCs generated in the southeastern WNP are stronger than TCs generated elsewhere. Generated in the southeastern WNP, TCs under El Niño atmospheric conditions (EAES and EALS, Figs. 3a and c) are stronger than TCs under La Niña atmospheric conditions (LALS and LAES, Figs. 3b and d). TCs under neutral conditions (Fig. 3e) are weaker than TCs under the rest of the conditions, except that TCs at 5°N in the eastern WNP are stronger than those TCs under La Niña conditions. Generated in the northern and western tropical WNP, TCs under La Niña conditions are stronger than TCs under the rest of the conditions. However, observations under each of the real conditions show that more than one TC may be generated in a particular location (Fig. 1); hence the variability of TC genesis rate should be considered. The genesis rates are calculated based on the JTWC best track data. The first TC location on record in the JTWC data is taken as the TC genesis location. TC genesis number (Fig. 4) in a $5^\circ \times 5^\circ$ box with the center of every location in Fig. 1 is counted for El Niño (Fig. 4a), La Niña (Fig. 4b), and neutral (Fig. 4c) years, respectively. In each of the boxes, TC genesis rate is defined as the genesis number divided by the total years under each of the conditions. There are more TCs generated in the southeastern tropical WNP and less TCs generated in the southwestern tropical WNP in El Niño years than in La Niña years. In neutral years, TCs are mainly generated in the central tropical WNP. This finding is consistent with the results of previous studies (e.g., Wang and Chan, 2002; Camargo et al., 2007a).

Observed TC genesis rates are then considered and combined with the modeled TC intensities. In each case (EAES, LALS, and NANS), the frequency of the modeled TC intensity in each location is simply multiplied by the observed genesis rate in each box in Fig. 4. For example, if the number in a box under El Niño conditions (Fig. 4a) is eight and the modeled TC intensity at this location in the corresponding experiment (EAES) is 19.8 m s^{-1}, 8 TCs with the intensity of 19.8 m s^{-1} are counted in EAES. Using this method, the frequency of the modeled TC intensity is counted in every box in each case (EAES, LALS, and NANS). The calculation of the genesis rate shows that the averaged TC intensity (Fig. 5a) decreased from 33.0 to 32.4 m s^{-1} in LALS, increased from 31.0 to 32.6 m s^{-1} in EAES, and increased from 30.3 to 31.2 m s^{-1} in NANS. The standard deviations of TC intensities become 5.4 m s^{-1} (EAES), 3.5 m s^{-1} (LALS), and 4.6 m s^{-1} (NANS). The mean intensity of the total modeled TCs becomes 32.0 m s^{-1}, with a standard deviation of 4.7 m s^{-1}. When the TC genesis rates are considered (Fig. 5b), the strong TCs ($\geqslant$32.0+4.7 m s^{-1}) in EAES are still more frequent than TCs in LALS, but the difference of frequency between EAES and LALS is larger than that when the genesis rate difference is not considered (Fig. 2b). Meanwhile, the frequency of TC intensity within 1 SD in LALS is decreasing compared with the case when the TC genesis rates are not considered. Overall, the TC genesis number (or rate) in each location has an important influence on the frequency of strong TCs. In other words, the more TCs generate in the southeastern WNP, the more TCs with strong intensities develop.

In Figs. 5c and d, the statistics of the observed TC intensities during June–November 1965–2009 are shown. In Fig. 5c, TC intensity range is large in neu-

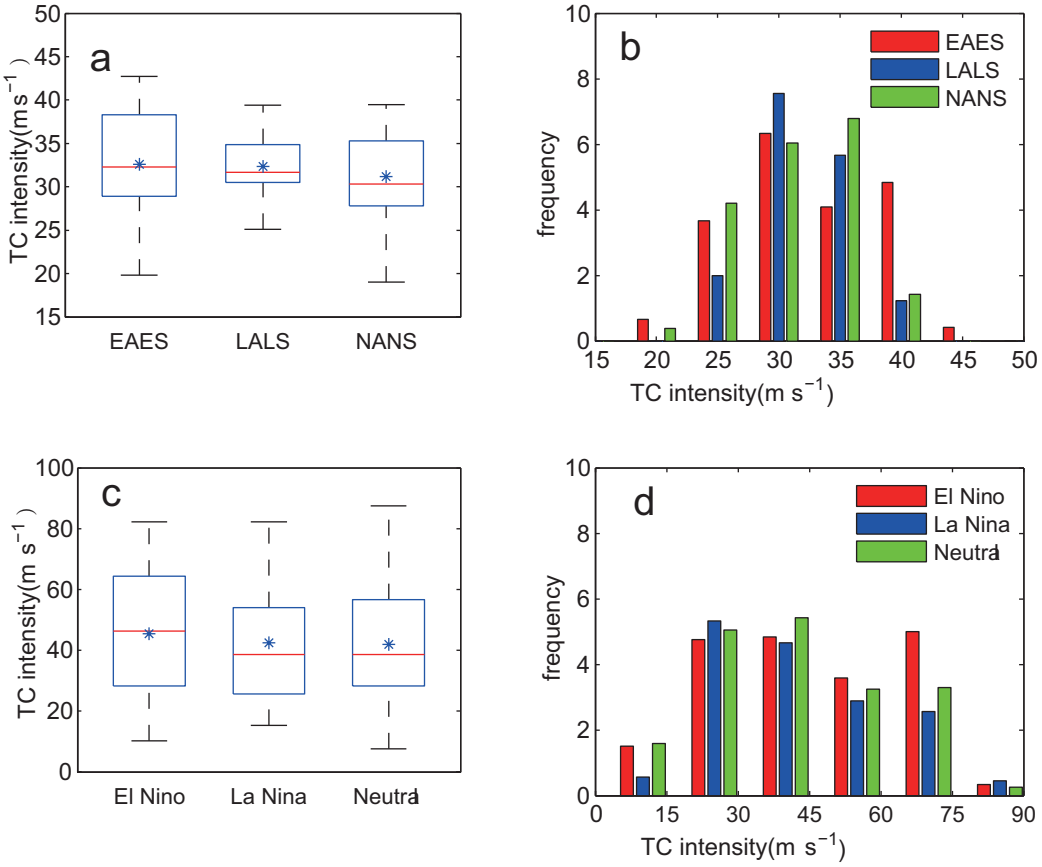

Fig. 5. Panels (a) and (b) are similar to Figs. 2a and b, but the TC genesis number and rate at each location (Fig. 4) are considered in the statistics of the TC intensities (see the text for details). Panels (c) and (d) are the corresponding boxplot and histogram of observed TC intensities, and (d) is the annual mean frequency. For panels (a) and (c), the x-axis and y-axis represent three cases and TC intensity respectively. For panels (b) and (d), the x-axis and y-axis represent TC intensity and frequency respectively.

tral years and small in La Niña years. The differences of average TC intensities among El Niño, La Niña, and neutral conditions are not significant. The mean intensity of the total observed TCs is 42.0 m s^{-1} with a standard deviation of 18.9 m s^{-1}. The frequency of strong TCs ($\geqslant$42.0+18.9 m s^{-1}) in El Niño years is more than TCs in La Niña years, as well as the weak TCs ($\leqslant$42.0–18.9 m s^{-1}). This result is in agreement with the model result.

TC intensities in the model experiments are smaller than the observations. This difference can be caused by two reasons. (1) The resolution is coarse in this study. TC intensity can increase by 6–10 m s^{-1} according to our tests with finer meshes (30 km), but the much longer time of integration is too costly. (2) This study focused on the effects of the time-mean atmospheric circulation on the TC intensity, so the circulation variability on the other time scales (e.g., MJO, Fudeyasu et al., 2010) is not considered. Variations on other time scales are also important for TC intensity changes and can modulate TCs to be stronger or weaker than those under the time-mean state circulation.

According to the intensity divisions in Fig. 5d (x-axis), the observed TC genesis locations and tracks are separated into six groups (Figs. 6 and 7) under El Niño, La Niña, and neutral conditions. The first three groups (Fig. 6) are for TCs with intensities of 0–15 m s^{-1}, 15–30 m s^{-1}, and 30–45 m s^{-1}. The other three groups (Fig. 7) are for TCs with intensities of 45–60 m s^{-1}, 60–75 m s^{-1}, and 75–90 m s^{-1}. TC tracks in each of the intensity groups cover almost the entire area of 5°–40°N, 110°–160°E, except the tracks in two groups: 0–15 m s^{-1} and 75–90 m s^{-1}. Observed TC intensity is also related to the genesis location. From weak intensity to strong intensity, TC frequency increased in the southeastern and central tropical WNP. In El Niño and neutral years, TCs generated in the

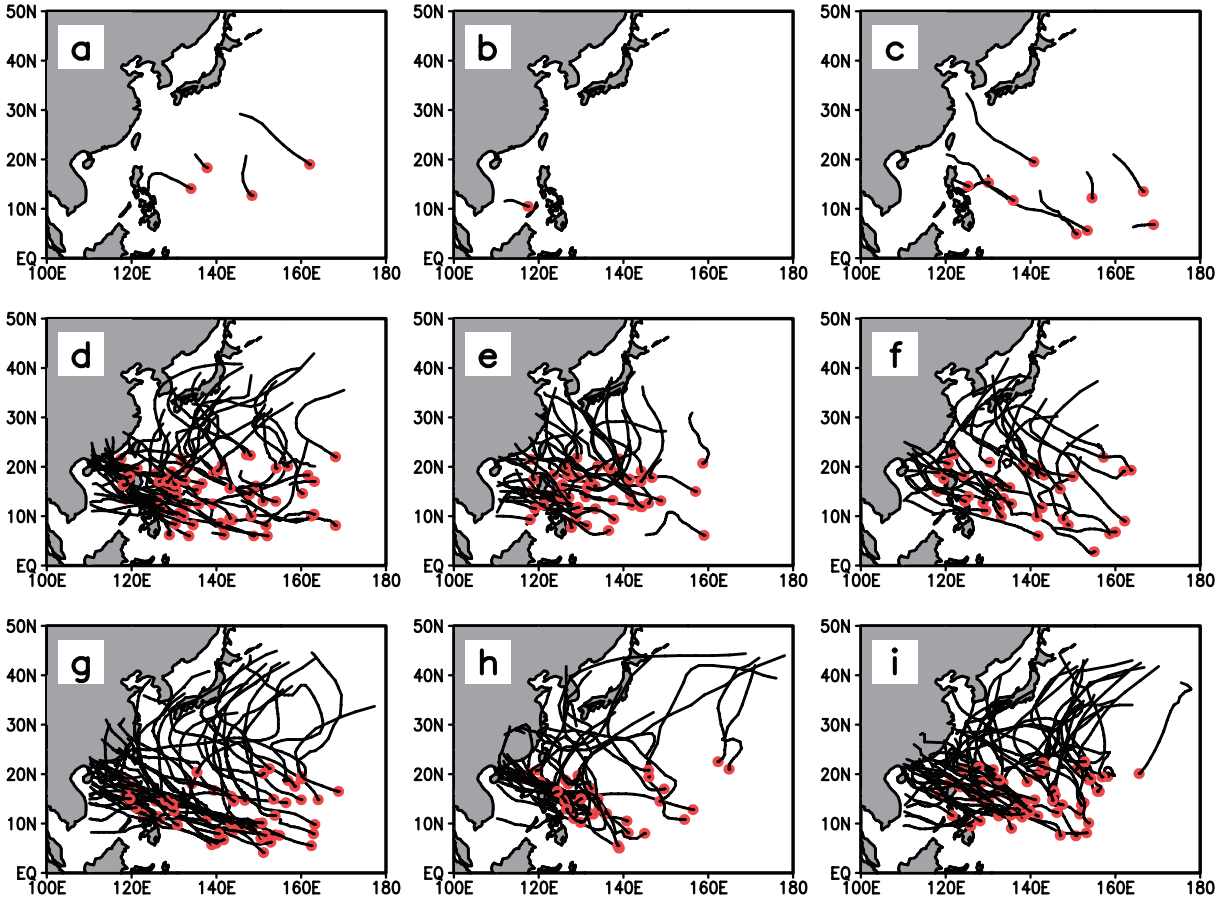

Fig. 6. Tracks and genesis locations of observed TCs with the intensities of 0–15 m s^{-1} (top row), 15–30 m s^{-1} (second row), 30–45 m s^{-1} (bottom row) in El Niño (left panels), La Niña (middle panels), and neutral (right panels) years.

southeastern and central tropical WNP are more frequent than those TCs in La Niña years.

Similarly, the modeled TC tracks (Fig. 8a) also cover the entirety of the observed TC track area in the WNP. When the TC genesis rates were considered in calculating the mean modeled TC tracks, similarity is found between the modeled and observed TC tracks (Figs. 8b and c). During El Niño years, the mean TC track is located east of the mean track for neutral years, whereas in La Niña years, the mean TC track is located west of the mean neutral track. This result resembles that of Camargo et al. (2007b), who analyzed observed TC tracks in WNP. They found that in El Niño years TCs are typically with the clustered in the eastern part of the WNP, whereas in La Niña years TCs are mostly with the clustered in the western part of the WNP. Furthermore, the TCs in the eastern WNP are stronger than those in the western WNP.

Overall, TCs generated in the southeastern WNP are stronger than those TCs generated elsewhere. TCs in the southeastern WNP under El Niño atmospheric conditions are stronger (and generated more) than those TCs under La Niña conditions. The genesis location has an important influence on the interannual variation of the TC intensity in the WNP. However, when the TC genesis rates are not considered (Fig. 3), TCs in the southeastern WNP in EAES are still stronger than those TCs in LALS. In the following subsection, the effects of the atmospheric factors on TC intensity are discussed.

3.2 *Dependence of TC intensity on environmental factors*

In the research of Gray (1968), the main environmental factors that are favorable for TC development are warm SST, small tropospheric vertical wind shear (VWS), cyclonic low-level relative vorticity (VOR), and large mid-tropospheric moisture content. In this study, we define the VOR as the mean relative vorticity of 1000–700 hPa; the VWS is defined as the absolute value of the zonal wind speed difference between 200 hPa and 850 hPa ($|u_{200} - u_{850}|$). The mid-

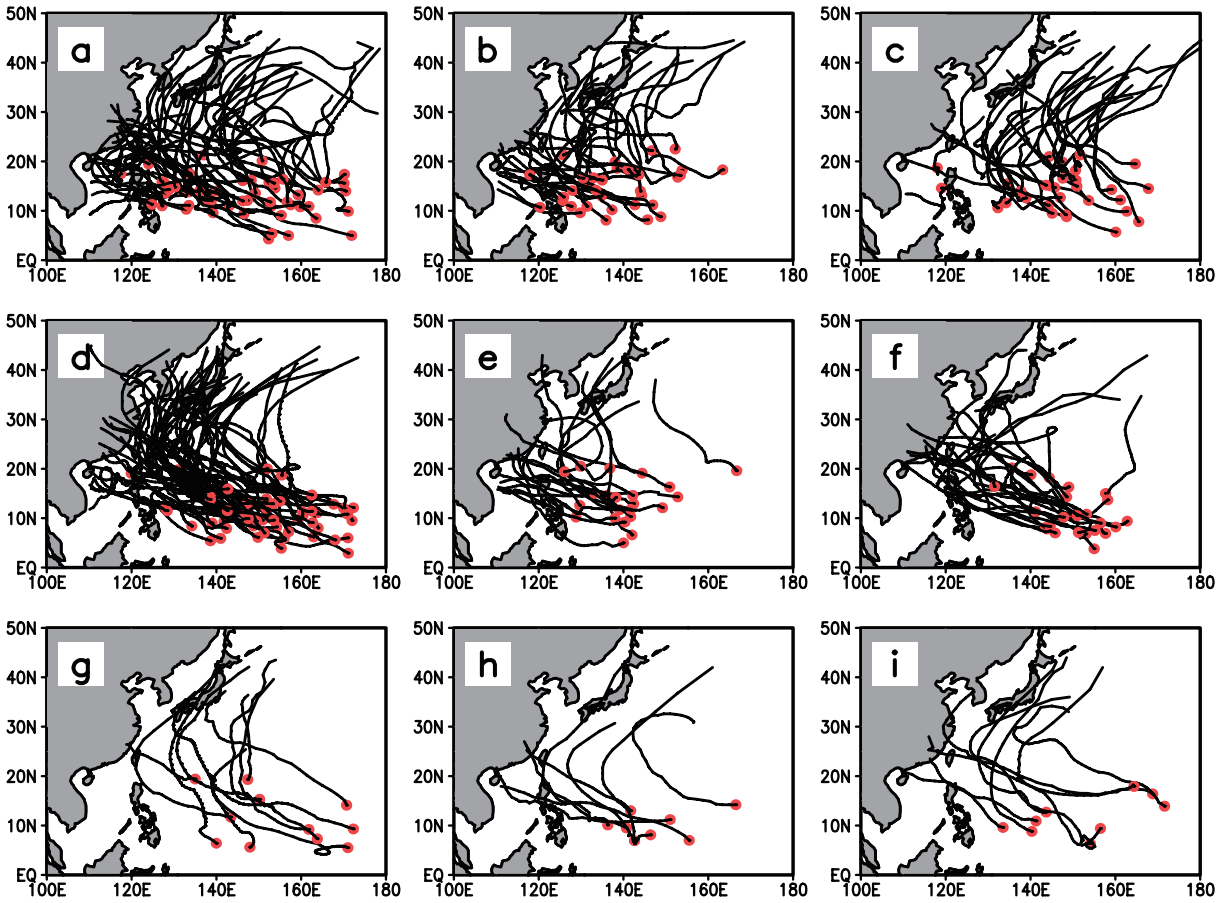

Fig. 7. Similar to Fig. 6 but for the TCs with the intensities of 45–60 m s^{-1} (top row), 60–75 m s^{-1} (second row), and 75–90 m s^{-1} (bottom row).

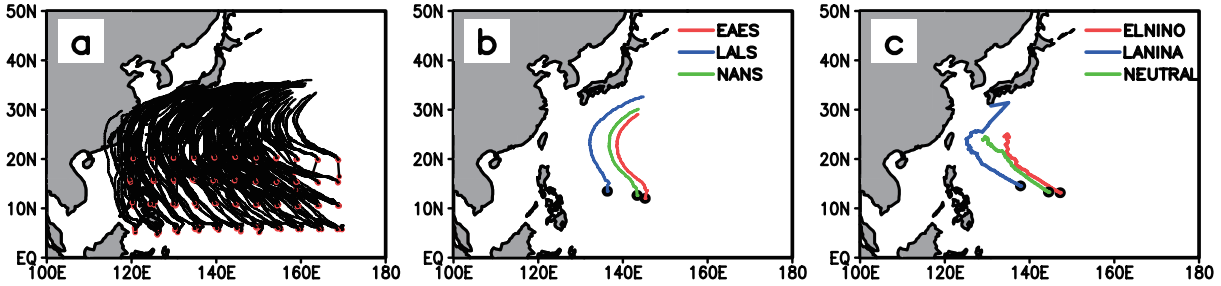

Fig. 8. (a) Tracks of 220 modeled TCs, (b) mean tracks of the modeled TC tracks but the real TC genesis rates (Fig. 4) are considered in each case (EAES, LALS and NANS), and (c) mean TC tracks from observations in El Niño, La Niña, and neutral years.

tropospheric moisture content is represented by the relative humidity (RHU) at 600 hPa according to Camargo et al. (2007a).

These factors in the model initial fields are shown in Fig. 9 for El Niño, La Niña and neutral years. The SST in El Niño years (Fig. 9a) is lower than that in La Niña years (Fig. 9b), except for the SST in the tropical area near the dateline. In both the El Niño and La Niña years, the VOR is positive at low latitudes and negative at middle latitudes (Figs. 9d and e). The magnitudes of the VOR in El Niño years are larger than those magnitudes in La Niña years. At low latitudes, small VWS is found near the dateline in El Niño years (Fig. 9g) and near 160°E in La Niña years (Fig. 9h). At middle latitudes, the VWS in El Niño years is stronger than that in La Niña years. In the western WNP, the RHU in El Niño years (Fig. 9j) is smaller than the RHU in La Niña years (Fig. 9k). In

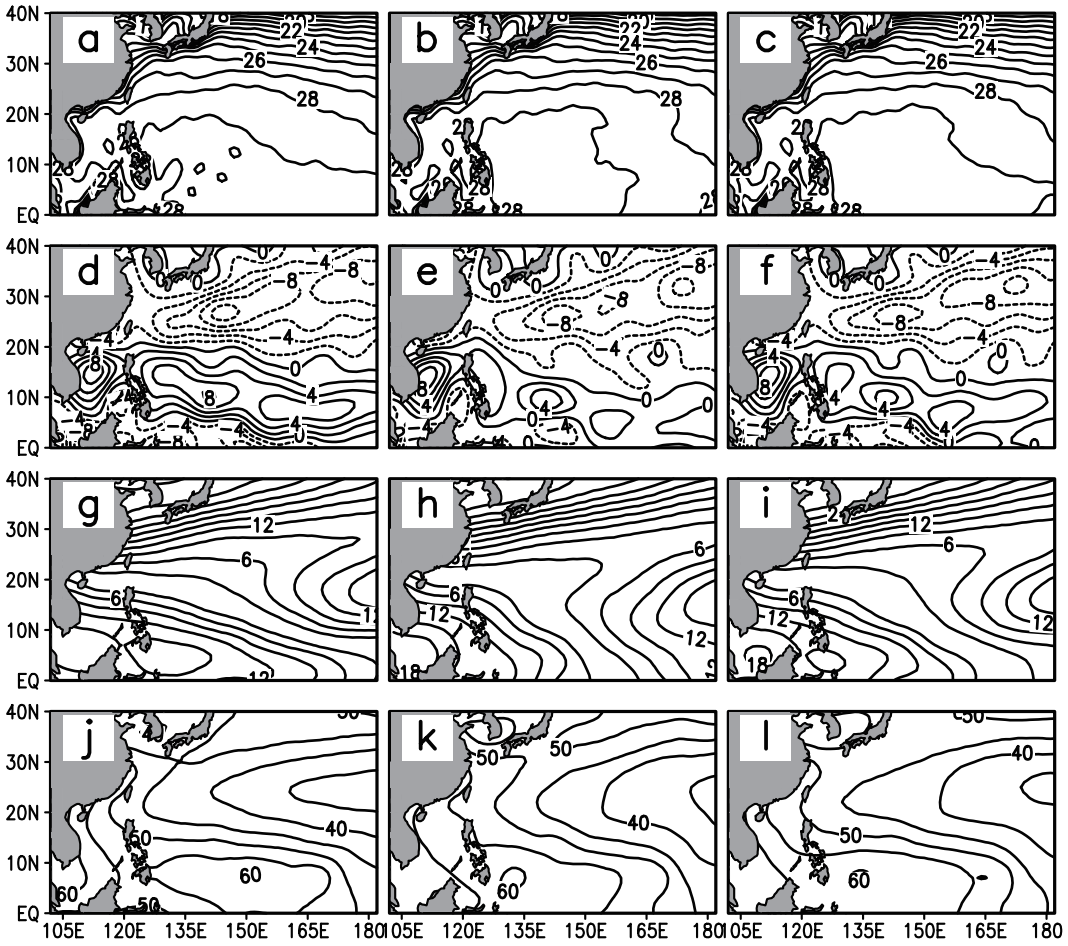

Fig. 9. Mean SST and atmospheric circulation fields (model initial fields) in El Niño (left panels), La Niña (middle panels), and neutral (right panels) years. SST (in °C, top row); low level vorticity (in 1×10^{-6} s^{-1}, second row); vertical wind shear (in m s^{-1}, third row); and relative humidity at 600 hPa (%, bottom row).

the eastern WNP, the RHU in El Niño years is larger than in La Niña years. In neutral years (Figs. 9c, f, i, and l), these fields exhibited distributions resembling the mean fields between El Niño and La Niña years.

The environmental factors in the initial fields have shown notable differences between El Niño, La Niña, and neutral conditions (Fig. 9). We further explore the dependence of the modeled TC intensities on these specific factors. For each modeled TC, we calculate the "along-track averages" of SST, VWS, VOR, and RHU based on the initial fields. At every time interval, each factor is first averaged in an area with a radius of 500 km from the center of a modeled TC and then averaged along the TC track before the TC reached the maximum intensity. This process is repeated for the 220 modeled TCs. Before using the "along-track averages", the variability of the atmospheric circulation in each experiment is quantified. For each experiment, we calculate the spatial correlation between the initial fields of the VWS, VOR, and RHU and their composite fields, respectively. The composites represent the averages during the beginning of the simulations to the time when TCs reach their maximum intensity. The spatial correlations between the initial and composite fields are 0.5 for VOR, 0.7 for RHU, and 0.9 for VWS. Although there is similarity between the initial and composite fields, the composite fields are not used to compute the "along-track averages" because the composite atmospheric fields are distorted by the modeled TCs.

The correlations between the intensities of the 220 modeled TCs and the corresponding "along-track averages" of SST, VWS, VOR and RHU are calculated. The TC intensity is significantly correlated with the SST (0.63), VWS (−0.59), and VOR (0.25) at the 5% significance level. At low latitudes, the SST is warmer, the VWS is smaller, and the VOR is larger than at middle latitudes (Fig. 9). Thus, TCs generated in the

southeastern WNP are subject to more favorable environmental conditions than TCs generated elsewhere.

The modeled TC intensity is not significantly correlated with the RHU because at the beginning of the simulations, the bogus TCs already have cyclonic structure (figure not shown) that is able to pump the wet air from the low troposphere up to the medium troposphere. Because of this "self-supporting" aspect, the development of the modeled TCs is not sensitive to the humidity. Previous studies (e.g., Camargo et al., 2007a) have shown that humidity is very important for the genesis of TCs in the WNP, but in this study the genesis process is not considered in the bogus TCs.

After analyzing the relationship between TC intensities and the "along-track averages" of SST, VWS, VOR, and RHU, we calculated the differences of these variables (denoted by Δ) between the experiments under El Niño (EAES) and La Niña (LALS) conditions. The correlations between the TC intensity difference and the environmental factor difference are 0.01 for the ΔSST, -0.27 for the ΔVWS, 0.53 for the ΔVOR, and 0.15 for the ΔRHU. The correlation with ΔVOR is at the 5% significance level, but the correlations with ΔSST, ΔVWS, and ΔRHU are not significant. These correlations imply that in addition to TC genesis location, VOR is another reason for more intense TCs in El Niño years. The large VOR in the WNP is closely associated to the monsoon trough, which can be identified by the axis of the large VOR centers (Lau and Lau, 1992; Wu et al., 2012).

The correlation between TC intensity and the "along-track averages" and the correlation between the difference of TC intensities and the differences of SST, VWS, VOR, and RHU (denoted by Δ) are not necessarily contradictory. The former is for all the 220 modeled TCs with different genesis locations, as well as different atmospheric and SST conditions. The latter shows the correlations between the differences of TC pairs with the same genesis locations. From both correlations, the model results suggest that (1) if TC genesis locations are different, the differences in SST, VWS and VOR all contribute to the differences in TC intensities; (2) if TCs generate in the same location, the difference in VOR is another primary factor causing TC intensity difference between El Niño and La Niña years.

4. Conclusions and discussions

The influence of TC genesis location and atmospheric circulation on the interannual variability of TC intensity in the WNP is explored using model sensitivity experiments. The model results suggest that TCs generated in the southeastern WNP are stronger than the TCs generated elsewhere, because the atmospheric circulation is more favorable for TC development at low latitudes than middle latitudes. In the observations, more TCs are generated in the southeastern WNP in El Niño years than in La Niña years. Thus, TCs in El Niño years have more chance to become intense than the TCs in La Niña years. Previous studies have pointed out that the atmospheric circulation in El Niño years is more favorable for the TC genesis in the southeastern WNP than the circulation in La Niña years. Camargo et al. (2007a) suggested that the mid-tropospheric humidity related to El Niño is one of the important factors for the annual genesis of TCs. In El Niño years, the monsoon trough in the WNP also provides favorable low-level vorticity for the TC genesis (Chen et al., 1998, 2004; Wu et al., 2012).

In addition to location of TC genesis, the monsoon trough also influences the TC intensity in the WNP. In the southeastern WNP, the modeled TCs under El Niño conditions are stronger than the TCs in La Niña years. For TCs generated in the same location, the difference of TC intensity between El Niño and La Niña conditions is significantly related to the VOR difference. Therefore, VOR is another important factor that influences the TC intensity difference between El Niño and La Niña years.

These model experiments have not fully demonstrated the effect of the SST on TC intensities because the feedback from SST on TC and the variation of SST are not considered in the experiments; these are important aspects associated with TC intensity. Therefore, experiments using coupled atmosphere-ocean model are needed to incorporate the feedbacks from SST on TC intensity.

In this study, model resolution is coarse and has a certain influence on the simulation of TC intensity. However, according to our fine-mesh (30-km) trial experiment (44 TCs in EAES), the resolution does not change the distribution of the intensity anomalies of the model TCs, and the fine-mesh study needs further work. The variance of the modeled TC intensities is small because in this study we focused on the effects of the mean-state circulation on TC intensity, and the circulations at the other scales are not considered (e.g., MJO). Those circulations can modulate the TCs to be stronger or weaker than TCs in the mean state circulation.

Acknowledgements. We acknowledge the support from the National Natural Science Foundation of China (NSFC: Grant No. 41175090 and 41175086). ZHOU Yang acknowledges the support from the NSFC (Grant No. 40975040), the Fundamental Research Funds for the Central Universities (Grant No. 1116020701), and "A Project

Funded by the Priority Academic Program Development of Jiangsu Higher Education Institutions." We thank the anonymous reviewers for their insightful and instructive comments.

REFERENCES

Betts, A. K., 1986: A new convective adjustment scheme. Part I: Observational and theoretical basis. *Quart. J. Roy. Meteor. Soc.*, **112**, 677–692.

Betts, A. K., and M. J. Miller, 1986: A new convective adjustment scheme. Part II: Single column tests using GATE wave, BOMEX, ATEX and Arctic air-mass data sets. *Quart. J. Roy. Meteor. Soc.*, **112**, 693–709.

Betts, A. K., and M. J. Miller, 1993: The Betts-Miller scheme. *The representation of cumulus convection in numerical models*, K. A. Emanuel and D. J. Raymond, Eds., Amer. Meteor. Soc., 246pp.

Camargo, S. J., and A. H. Sobel, 2005: Western North Pacific tropical cyclone intensity and ENSO. *J. Climate*, **18**, 2996–3006.

Camargo, S. J., K. A. Emanuel, and A. H. Sobel, 2007a: Use of genesis potential index to diagnose ENSO effects on tropical cyclone genesis. *J. Climate*, **20**, 4819–4834.

Camargo, S. J., A. W. Robertson, S. J. Gaffney, P. Smyth, and M. Ghil, 2007b: Cluster analysis of typhoon tracks. Part Ⅱ: Large-scale circulation and ENSO. *J. Climate*, **20**, 3654–3676.

Chan, J. C. L., 1985: Tropical cyclone activity in the northwest Pacific in relation to the El Niño/southern oscillation phenomenon. *Mon. Wea. Rev.*, **113**, 599–606.

Chan, J. C. L., 2008: Decadal variations of intense typhoon occurrence in the western North Pacific. *Proc. Roy. Soc. London*, **464**, 249–272.

Chan, J. C. L., and K. S. Liu, 2004: Global warming and western North Pacific typhoon activity from an observational perspective. *J. Climate*, **17**, 4590–4602.

Chen, T. C., S. P. Weng, N. Yamazaki, and S. Kiehne, 1998: Interannual variation in the tropical cyclone Formation over the western North Pacific. *Mon. Wea. Rev.*, **126**, 1080–1090.

Chen, T. C., S. Y. Wang, and M. C. Yen, 2004: Role of the monsoon gyre in the interannual variation of tropical cyclone formation over the western north pacific. *Wea. Forecasting*, **19**, 776–785.

Dudhia, J., 1989: Numerical study of convection observed during winter monsoon experiment using a mesoscale two-dimensional model. *J. Atmos. Sci.*, **46**, 3077–3101.

Frank, W. M., and E. A. Ritchie, 1999: Effects of environmental flow upon tropical cyclone structure. *Mon. Wea. Rev.*, **127**, 2044–2061.

Frank, W. M., and E. A. Ritchie, 2001: Effects of vertical wind shear on the intensity and structure of numerically simulated hurricanes. *Mon. Wea. Rev.*, **129**, 2249–2269.

Fudeyasu, H., Y. Wang, M. Satoh, T. Nasuno, H. Miura, and W. Yanase, 2010: Multiscale interactions in the life cycle of a tropical cyclone simulated in a global cloud-system-resolving model. Part I: Large-scale and storm-scale evolutions. *Mon. Wea. Rev.*, **138**, 4285–4304.

Gray, W. M., 1968: Global view of the origin of tropical disturbances and storms. *Mon. Wea. Rev.*, **96**, 669–700.

Hong, S. Y., and H. L. Pan, 1996: Nonlocal boundary layer vertical diffusion in a medium-range forecast model. *Mon. Wea. Rev.*, **124**, 2322–2339.

Huang, P., C. Chou, and R. Huang, 2011: Seasonal modulation of tropical intraseasonal oscillations on tropical cyclone geneses in the western North Pacific. *J. Climate*, **24**, 6339–6352.

Iizuka, S., and T. Matsuura, 2008: ENSO and western North Pacific tropical cyclone activity simulated in a CGCM. *Climate Dyn.*, **30**, 815–830.

Janjic, Z. I., 1994: The step-mountain eta coordinate model: Further development of the convection, viscous sublayer, and turbulent closure schemes. *Mon. Wea. Rev.*, **122**, 927–945.

Kalnay, E. M. Kanamitsu, and R. Kistler, 1996: The NCEP/NCAR 40-year reanalysis project. *Bull. Amer. Meteor. Soc.*, **77**, 437–471.

Kistler, R. E. Kalnay, and W. Collins, 2001: The NCEP-NCAR 50-year reanalysis: Monthly means CD-ROM and documentation. *Bull. Amer. Meteor. Soc.*, **82**, 247–267.

Lander, M. A., 1993: Comments on "AGCM simulation of the relationship between tropical-storm formation and ENSO". *Mon. Wea. Rev.*, **121**, 2137–2143.

Lander, M. A., 1994: An exploratory analysis of the relationship between tropical storm formation in the western North Pacific and ENSO. *Mon. Wea. Rev.*, **122**, 636–651.

Lau, K.-H., and N.-C. Lau, 1992: The energetics and propagation dynamics of tropical summertime synoptic-scale disturbances. *Mon. Wea. Rev.*, **120**, 2523–2539.

Liu, Y., D. L. Zhang, and M. K. Yau, 1997: A multiscale numerical study of hurricane Andrew (1992). Part I: Explicit simulation and verification. *Mon. Wea. Rev.*, **125**, 3073–3093.

Liu, Y., D. L. Zhang, and M. K. Yau, 1999: A multiscale numerical study of hurricane Andrew (1992). Part II: Kinematics and inner-core structures. *Mon. Wea. Rev.*, **127**, 2616–2597.

Lownam, S., and C. Davis, 2001: Development of a tropical cyclone bogussing scheme for the MM5 system. Preprint, *the Eleventh PSU/NCAR Mesoscale Model Users' Workshop*, Boulder, Colorado, 130–134.

Matsuura, T., M. Yumoto, and S. Iizuka, 2003: A mechanism of interdecadal variability of tropical cyclone activity over the western North Pacific. *Climate Dyn.*, **21**, 105–117.

Pielke Jr., R. A., and C. N. Landsea, 1999: La Niña, El Niño, and Atlantic hurricane damages in the United

States. *Bull. Amer. Meteor. Soc.*, **80**, 2027–2033.

Sobel, A. H., and E. D. Maloney, 2000: Effect of ENSO and MJO on the western North Pacific tropical cyclones. *Geophys. Res. Lett.*, **27**, 1739–1742.

Trenberth, K. E., 1997: The definition of El Niño. *Bull. Amer. Meteor. Soc.*, **78**, 2771–2777.

Wang, B., and J. C. L. Chan, 2002: How strong ENSO events affect tropical storm activity over the western North Pacific. *J. Climate*, **15**, 1643–1658.

Wang, S. Y., and A. J. Clark, 2010: Quasi-decadal spectral peaks of tropical western Pacific SSTs as a precursor for tropical cyclone threat. *Geophys. Res. Lett.*, **37**, L21810, doi: 10.1029/2010GL044709.

Wong, M. L. M., and J. C. L. Chan, 2004: Tropical cyclone intensity in vertical wind shear. *J. Atmos. Sci.*, **61**, 1859–1876.

Wu, L., Z. P. Wen, R. H. Huang, and R. G. Wu, 2012: Possible linkage between the monsoon trough variability and the tropical cyclone activity over the western North Pacific. *Mon. Wea. Rev.*, **140**, 140–150.